crystals

MDPI

Article

Mn-Ce Oxide Nanoparticles Supported on Nitrogen-Doped Graphene for Low-Temperature Catalytic Reduction of NO_x: De-Nitration Characteristics and Kinetics

Shangrong Tan [1], Zhuo Yao [1,*], Hong Huang [2,*], Feng Liu [1], Zechen Liu [1] and Xuyuan Wang [3]

[1] Collage of Materials and Metallurgy, University of Science and Technology Liaoning, Anshan 114001, China
[2] Department of Mechanical and Materials Engineering, Wright State University, Dayton, OH 45435, USA
[3] Zhengzhou Ruitai Refractory Materials Technology Co., Ltd., Zhengzhou 452374, China
* Correspondence: yaozhuo1986@163.com (Z.Y.); hong.huang@wright.edu (H.H.)

Abstract: Selective catalytic reduction (SCR) of NO_x with NH_3 as the reductant has been proven an efficient and cost-effective technology to remove NO_x pollutants in industries. Traditional SCR catalysts usually operate above 300 °C and suffer from intoxication and limited lifetime. Nano-catalysts are attractive for their high catalytic activities at reduced operating temperatures. We have recently developed a series of nitrogen-doped graphene-supported Mn-Ce oxides ($MnCeO_x$/NG). The influences of reaction temperature, space velocity, mole ratio of NH_3/NO and O_2 concentration on SCR de-nitration activity were assessed. The novel catalyst with optimal Mn/Ce ratio, at appropriate processing conditions, can achieve a NO conversion efficiency of 99.5% at a temperature of 180 °C, and 93.5% at 150 °C. The kinetics of the SCR reaction on this novel catalyst were also established, exhibiting first-order with respect to NO, zero-order to NH_3, and nearly 0.5-order to O_2 at low temperatures. In the presence of sufficient O_2 content, the apparent activation energy of the NH_3-SCR on $MnCeO_x$/NG is 37.6 kJ/mol, which is promising for low-temperature applications.

Keywords: NH_3-SCR; kinetics; catalyst; N-doped graphene; $MnCeO_x$ nanocomposite

check for updates

Citation: Tan, S.; Yao, Z.; Huang, H.; Liu, F.; Liu, Z.; Wang, X. Mn-Ce Oxide Nanoparticles Supported on Nitrogen-Doped Graphene for Low-Temperature Catalytic Reduction of NO_x: De-Nitration Characteristics and Kinetics. *Crystals* **2023**, *13*, 313. https://doi.org/10.3390/cryst13020313

Academic Editor: Bo Chen

Received: 30 January 2023
Revised: 8 February 2023
Accepted: 12 February 2023
Published: 14 February 2023

Copyright: © 2023 by the authors. Licensee MDPI, Basel, Switzerland. This article is an open access article distributed under the terms and conditions of the Creative Commons Attribution (CC BY) license (https://creativecommons.org/licenses/by/4.0/).

1. Introduction

Nitrogen oxides (NO_x) in air have attracted global attention because they lead to serious environmental problems such as acid rain, photochemical smog, ozone depletion, greenhouse effects, etc. Among various de-NO_x technologies, selective catalytic reduction of NO_x with NH_3 (NH_3-SCR) as the reductant has been proven an efficient and cost-effective technology, and widely applied on stationary source combustion units. The catalyst is the key to achieving a high efficiency of removal of NO_x in NH_3-SCR. However, present industrial SCR catalysts such as V_2O_5-WO_3/TiO_2 only function effectively within a temperature window of 300–400 °C. As a consequence, the SCR-catalyst system has to be installed before the dust collector and desulfurization tower, in order to surpass the threshold for the catalyst being activated [1–4]. The narrow operating temperatures of these catalysts exclude their applications in steel and cement plants wherein the flue gas is usually less than 250 °C. Novel catalysts with high SCR activity at lower operating temperatures will present enormous economic and environmental impacts.

Transition metal oxide-based catalysts have exhibited superior low-temperature NO_x conversion efficiency. Among them, manganese oxides (MnO_x) are attractive candidates due to their abundant resource, environmental friendliness and low cost. The surface of MnO_x is known to have a significant amount of labile oxygen, which plays a vital role in the catalytic cycle of SCR reactions at low temperatures [5–8]. Ceria (CeO_2) has also been confirmed as potential active catalyst as well as an effective promoter/supporter for enhancing the catalytic activity of various materials. In ceria, oxygen can be stored and released through the redox shift between Ce^{4+} and Ce^{3+}, promoting the fast SCR reaction [9].

When mixing MnO_x with CeO_2, the SCR catalytic activities were further enhanced [6,7,9]. Qi et al. reported that MnO_x-CeO_2 composites exhibited extraordinary low-temperature NH_3-SCR activity, with over 95% NO conversion efficiency on MnO_x(0.4)-CeO_2(500) at a temperature of 150 °C and a gas flow of GHSV = 42,000 h^{-1} [10].

Appropriate supporters for catalysts can not only provide an appropriate surface for good distribution of the active catalyst and prevention of large particles' generation, but can also add extra sites or charge transfers to enhance the catalytic reduction. Different supporters for SCR catalysts with have been reported, such as TiO_2 [11–14], γ-Al_2O_3 [15–17], CNTs [18–20], graphene [21,22], graphene aerogel [23], and TiO_2-graphene [24]. Zhao reported that MnO_x-CeO_2 (10:1) supported on TiO_2 with 1% NG exhibited the highest SRC efficiency and improved tolerance to SO_2 at 160 °C [25]. Compared with oxide supporters, graphene nanosheets have numerous merits, such as extremely high surface area, high electronic mobility, chemical stability, hydrophobicity, and stability of anchoring nano catalysts, etc. In our previous study [23], the SCR performance of an MnO_x-CeO_2 catalyst supported on three-dimensional graphene aerogel exhibited over 90% NO_x conversion rate within a broad temperature range (200–300 °C). Graphene nanosheets can be doped with foreign atoms, and their electrical and chemical properties can be tuned. In nitrogen-doped graphene (NG), nitrogen atoms can form two more bonding structures, i.e., pyridinic and pyrrolic, besides the graphitic, which causes distortion of graphene symmetry and/or extra vacancy sites in the vicinity [26]. The unique bonding configurations in N-doped graphene lattices render some distinct surface properties. It was reported that the incorporation of N into the graphene network can facilitate adsorption and bond cleavage of O_2, promoting an oxygen reduction reaction [27,28]. Recently, we have synthesized a series of nitrogen-doped graphene supported Mn-Ce oxide nanocomposites ($MnCeO_x$/NG) which have not been found in the public literature. Moreover, we have investigated the impact of concentrations of NO, NH_3 and O_2 on NH_3-SCR's denitrification, and established its reaction kinetics using a novel $MnCeO_x$/NG catalyst in the absence of any oxide carriers.

2. Experiment Aspect

2.1. Synthesis of Nitrogen Doped Graphene Supporters (NG)

In this study, a low-cost modified Hummers approach was used to prepare graphene oxides (GO) [29,30]. Typically, sodium nitrite and graphite were combined with strong sulfuric acid. The mixture was then gradually supplemented with potassium permanganate, which was then agitated in a water bath at 35 °C. Hydrogen peroxide was gradually added to the mixture after two hours, until the mixture's color turned brilliant yellow. The powders were then filtered and washed using deionized (DI) water and diluted hydrochloric acid (10 wt%) until the pH value reached about 7. The resulting GO powders were thoroughly dried in a vacuum furnace at 60 °C overnight. Afterwards, pyrrole was gradually added to a GO/water suspension solution and agitated for 0.5 h, followed by adding $FeCl_3$ solution. The reaction was maintained at 0 °C under constant stirring for 7 h. The product was washed with ethanol and DI water, and then dried at 60 °C for 12 h under vacuum. The resulting powders were further annealed at 800 °C in a tube furnace with flowing argon gas. The annealing process removed a significant amount of oxygen from the graphene; meanwhile, it accelerated nitrogen doping into the graphene lattice, leading to the formation of nitrogen-doped graphene nanosheets (NG).

2.2. Synthesis of NG-Supported Manganese and Cerium Oxide Composites

The as-synthesized NG powders were dispersed in DI water at a concentration of 2 mg/mL and sonicated for 30 min. A solution with pre-determined amount of manganese acetate $Mn(CH_3COO)_2$ and cerium nitrate $(Ce(NO_3)_2$ was then added dropwise while continuously stirring. The pH value of the solution was adjusted to 10 by adding a certain amount of ammonia. Such a suspension solution was continuously stirred at 80 °C for 1h in a water bath. The solution was then transferred into a stainless steel autoclave. The thermal reaction was set at 160 °C for 12 h. The products were filtered, washed, and dried.

Finally, the as-prepared powders were annealed at 400 °C for 2 h in argon atmosphere at a ramping rate of 10 °C/min.

The nitrogen-doped graphene-supported catalyst was named Mn(X)Ce(Y)/NG, in which NG represents the nitrogen-doped graphene as a carrier, X the weight percentage loading of MnO_x, and Y the molar ratio of Mn/Ce molar ratio. We have synthesized a series of the Mn(X)Ce(Y)/NG powders. Their structural and topological properties as well as their SCR performances have been systematically characterized. The results will be published elsewhere. In this paper, we will focus on the SCR kinetic study and performance of Mn10Ce41/NG synthesized at 400 °C, which is the best among the series.

2.3. SCR-Reactor and Reaction Conditions

A self-designed quartz tube fixed-bed test bench was used to test the SCR denitrification activity and the reaction kinetics of the catalysts. The system has an integral reactor for the steady-state experiment and a differential reactor for the transient experiment. NO, N_2 and O_2 were used to simulate industrial flue gas, and NH_3 was used as the reducing agent. The concentrations and flow rate of the simulated flue gases were controlled by mass flow meters. The tubing of the reactor system was heat-traced to prevent formation and deposition of ammonium nitrate. An ammonia trap containing phosphoric acid solution was installed before the sample entrance to the chemiluminescent analyzer in order to avoid inaccuracies caused by the oxidation of ammonia in the converter of the NO/NO_x analyzer. The catalyst was heated to 400 °C for 30 min in flowing Ar before each experiment. A chemiluminescent NO/NO_x analyzer was used to continuously track the amounts of NO and NO_2 (Thermo Environmental Instruments Inc., Franklin, MA, USA, Model 42C). The NO conversion efficiency was calculated based on Equation (1):

$$\text{NO conversion } (\%) = \frac{[\text{NO}]_{in} - [\text{NO}]_{out}}{[\text{NO}]_{in}} \times 100\% \quad (1)$$

2.3.1. Kinetic Studies

The first set of experiments are performed to determine reaction order and conducted in the differential reactor. To determine the reaction order for NO, the concentration of NO was changed within the range of 200–1000 ppm, while the concentration of NH_3 was kept at 1000 ppm and O_2 at 3%. Similarly, when studying the reaction order of NH_3, the concentration range of NH_3 was 400–1000 ppm, while the NO and O_2 concentrations were maintained at 1000 ppm and 3%, respectively. In order to determine the reaction order of O_2, the concentration of O_2 ranged from 0~5%, while the concentrations of NO and NH_3 were both kept at 1000 ppm. Three temperatures were selected: 150, 180, 210 °C.

To determine the reaction rate in relation to reactant concentrations, the impact of diffusion and transfer of reactants needs to be minimized; this can be accomplished at a large gas flow rate on a small amount of the catalyst [31]. In this study, the total gas flow rate was 3000 mL/min, and 50 mg of the catalyst was used. The ratio of the mass of the catalyst over the flow rate is 1g s/L, which limited the denitrification efficiency in the SCR reaction to below 20% and does not change with the flow rate.

The second set of experiments are conducted in the integral reactor. The flue gas flow rate was controlled at 1000 mL/min. The catalyst amount was 50, 100, 200, 400 and 700 mg, respectively. Flue gas composition was set as 500 ppm NO, 500 ppm NH_3, 3% O_2, balance with Ar. The temperatures tested are 150 °C, 180 °C and 210 °C. In the presence of sufficient O_2, the apparent activation energy of NO reduction is determined.

2.3.2. De-Nitration Performance Assessment

In the SCR catalyst activity test, a catalyst volume of 2 mL was used. The simulation flue gas is made up of 500 ppm NO, NH_3, O_2, and the balance gas was Ar. To determine the optimal reduction conditions, the impacts of the concentration of oxygen (0.05–5%), the concentration of NH_3 (molar ratio of $n_{[NH3]}/n_{[NO]}$), and the gas hourly space velocity

(GHSV) on the nitrogen conversion efficiency were determined. The GHSV of 2×10^6 h^{-1} is equivalent to 3000 mL/min.

3. Results and Discussion

Figure 1 shows the NO conversion in transient response to NH_3 and O_2 at 150 °C in the presence of the novel NG-Mn10Ce41 catalyst. As seen in Figure 1, when the NH_3 supply is turned off, the NO conversion decreases rapidly and lowest equilibrium NO conversion efficiency in the absence of NH_3 is 13.5%. Upon re-feeding the NH_3 into the flue gas (NO + O_2 + Ar), two-step processes are observed. Initially, the NO removal rate maintained its lowest level. After a certain period, the NO conversion rate started to take off and rose rapidly. However, the conversion reached a saturation efficiency of 84%. It is noteworthy that after the NH_3 off–on cycle, the NO conversion efficiency is not fully recovered, and is lower than the initial value. For the NH_3-SCR process, there are two distinguished reaction mechanisms, i.e., the Langmuir–Hinshelwood (L–H) mechanism and Eley–Rideal (E–R) mechanism. It is reported that the L–H mechanism is dominant on MnO_x-CeO_2 based catalysts, where NO and O_2 are readily adsorbed followed by electron transfer. Accordingly, NO would be converted into large amounts of nitrate and nitrite species [32], covering on the catalyst surface. At the initial stage of re-introducing NH_3, NH_3 cannot absorb on catalyst surface to assist NO reduction due to the lack of active sites, resulting in a very low SCR conversion rate. With the gradual N_2 formation and release from catalyst surface, some active sites become available for NH_3 absorption. When NH_3 reaches a sufficient level, the catalytic reaction takes off and conversion efficiency increases rapidly. However, the excessive nitrate and nitrite in the absence of NH_3 will poison a portion of active sites on the catalyst surface, which can be attributed to the decrease in denitrification efficiency. On the other hand, when O_2 was cut off from the reaction gas, the NO conversion decreased slowly and reached 8% at the steady state. When O_2 was reintroduced into the system, the NO conversion efficiency rapidly increased and recovered its initial value. Oxidation state of Mn and Ce as well as the activated chemisorbed oxygen species on the catalyst surface is critical in the SCR reaction [33]. Kinetically, removal of chemisorbed oxygen from catalyst surface will be much slower than removal physically adsorbed NH_3 gas. Hence, it took a longer time to terminate the NO conversion. In the absence of O_2, NO conversion on Mn10Ce41/NG is about half of that in the absence of NH_3; manifesting O_2 is more important than NH_3 in the SCR reaction, which is consistent with the kinetic analyses. As O_2 is reintroduced into the system, chemisorbed oxygen is rapidly recovered on the catalyst surface, promoting rapid SCR, and the process is completely reversible.

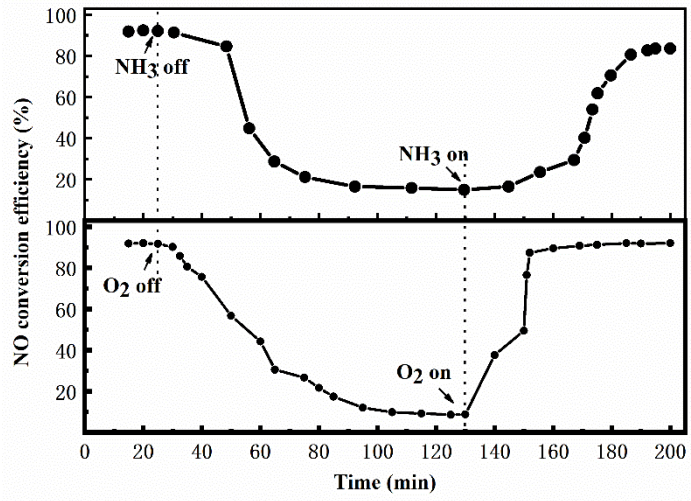

Figure 1. Transient response at 150 °C with NH_3 and O_2 on–off, showing the de-nitration on the novel Mn10Ce41/NG catalyst.

To fundamentally understand the above transient response of the denitration reaction on Mn10Ce41/NG, we investigate the reaction kinetics. For the simulated flue gas, the standard NH_3-SCR reaction is as the following:

$$4\,NO + 4\,NH_3 + O_2 = 4\,N_2 + 6\,H_2O \quad (2)$$

Its reaction rate as a function of the reactant concentrations can be expressed as:

$$R_{NO} = -k[NO]^x[NH_3]^y[O_2]^z \quad (3)$$

where k is a rate constant, x, y, z, are the reaction order for individual reactant gas A (A = NO, NH_3, or O_2). The denitrification rate of NG-Mn10Ce41 catalysts in relation to the concentration of NO, NH_3, and O_2 in the temperature range of 150–210 °C is shown in Figure 2. The linear relationships between ln R_{NO} and ln [A] are apparent, as seen in Figure 2b,d,e, and the corresponding reactor order can be determined from the slope.

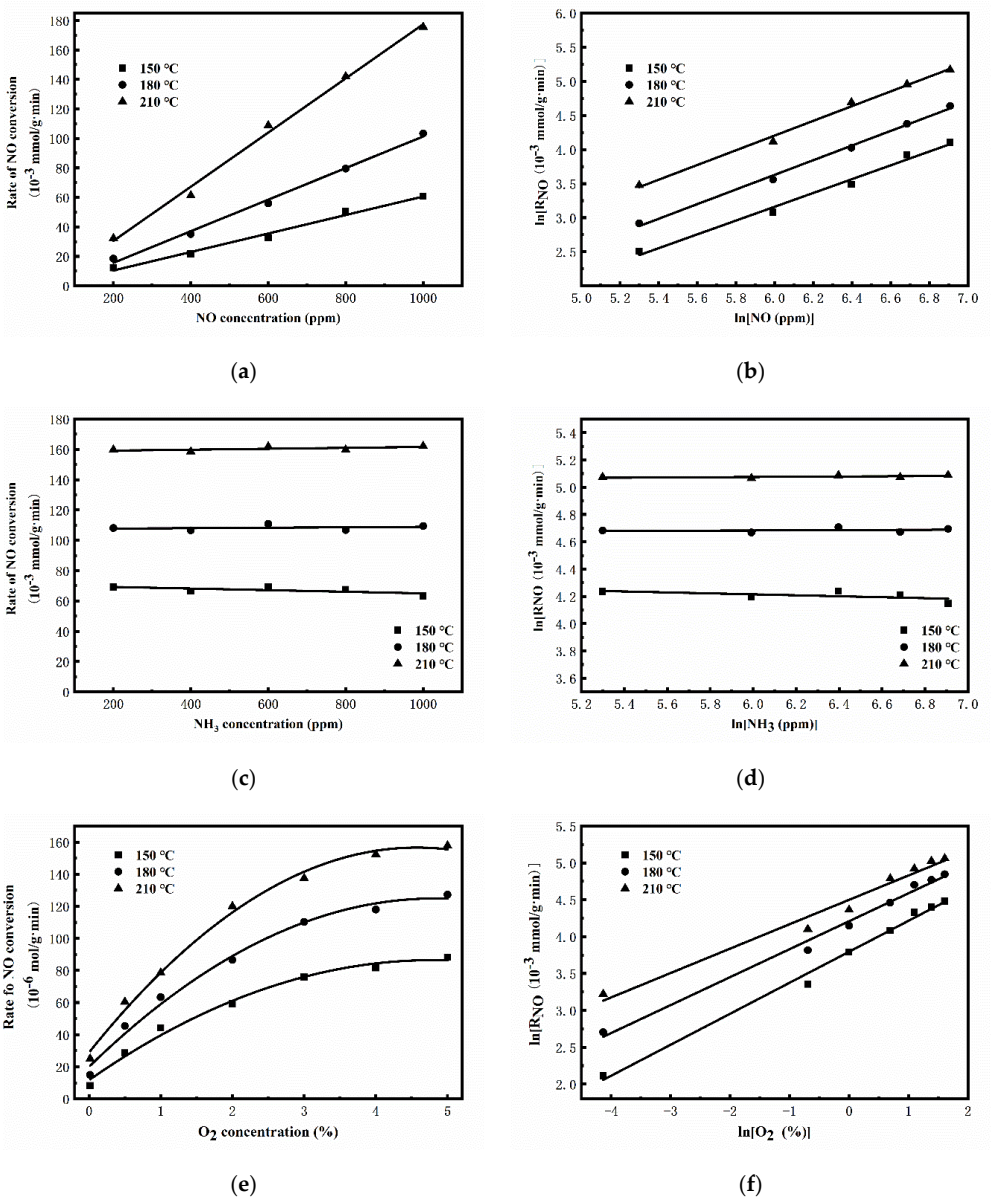

Figure 2. NO conversion rate as a function of concentration of NO (**a**,**b**), NH_3 (**c**,**d**), O_2 (**e**,**f**) in linear and corresponding logarithmic scales. The other reaction conditions are fixed at 50 mg of catalyst, 3000 mL/min of total flow rate, and temperatures 150–210 °C.

It is found in this study that SCR reaction orders on the Mn10Ce41/NG nanocatalyst composites, with respect to NO and NH_3 are 1 and 0, respectively; this is consistent with previous results (with no supporter/carrier, Qi 2004 [10]). Seen in Figure 2e, the slopes of log R_{NO}–n_{O2} plots were fitted as 0.420, 0.375, and 0.343 at 150 °C, 180 °C, and 210 °C, respectively. Our results suggest that reaction order of O_2 is close to 1/2 at lower temperatures, but gradually transitioned to 1/3 as the temperature increased to around 200 °C. By contrast, on microcrystalline MnO_x-CeO_2, approximately one-half order with respect to O_2 was reported. Based on the above analyses, it is proposed that the L-H mechanism is controlling the kinetics of NH_3-SCR on the Mn10Ce41/NG catalysts in the temperature range of 150 °C to 210 °C. The reaction rate can be expressed as the following:

$$\text{Around } 150\ ^\circ\text{C}: \ R_{NO} = -k[NO][O_2]^{1/2} \tag{4}$$

$$\text{Around } 210\ ^\circ\text{C}: \ R_{NO} = -k[NO][O_2]^{1/3} \tag{5}$$

The oxidation state on the surface of the oxide catalyst is critical in the SCR reaction [33]. Both chemisorbed and lattice oxygens exist on the catalyst surface, which can promote the SCR reaction. At low temperatures around 150 °C, a large amount of chemisorbed oxygen on the Mn10Ce41/NG catalyst readily reacts with NH_3 and NO. As the temperature increases, e.g., at 210 °C, oxygen absorption on catalyst could be lessened when the lattice oxygen in the catalyst (MnO_x and CeO_2) can become dominant within the SCR kinetics, leading to a change of the oxygen order in the kinetics.

Seen in Figure 2e, when the O_2 concentration was more than 3%, the NOx conversion tends to level-off and changes insignificantly. At such condition, the reaction rate of NO conversion can be rewritten as

$$R^*_{NO} = k^*[NO] \tag{6}$$

The apparent reaction rate constant (k*) can be obtained as the following,

$$k^* = -\frac{F_0 \ln(1-x)}{W} \tag{7}$$

where x is the NO removal rate, F_0 is the gas flow rate, W is the mass of catalyst. Table 1 lists the NO conversion efficiency at the three temperatures using different amounts of catalysts. Figure 3a plots the variation of $-\ln(1-x)$ with W/F_0 at different temperatures, showing the linear relationship. From the slope, the apparent reaction rate constant (k*) at each temperature is determined. Based on the Arrhenius equation,

$$k^* = k^*_o e^{-E_a/RT} \tag{8}$$

Table 1. SCR activity in an integral reactor.

Catalyst Amount (mg)	NO Conversion at Different Temperatures (%)		
	150 °C	**180 °C**	**210 °C**
50	2.6	5.1	9.6
100	6.2	12.6	17.6
200	8.7	19.1	35.5
400	19.8	34.5	54.6
700	31.6	54.2	76.3

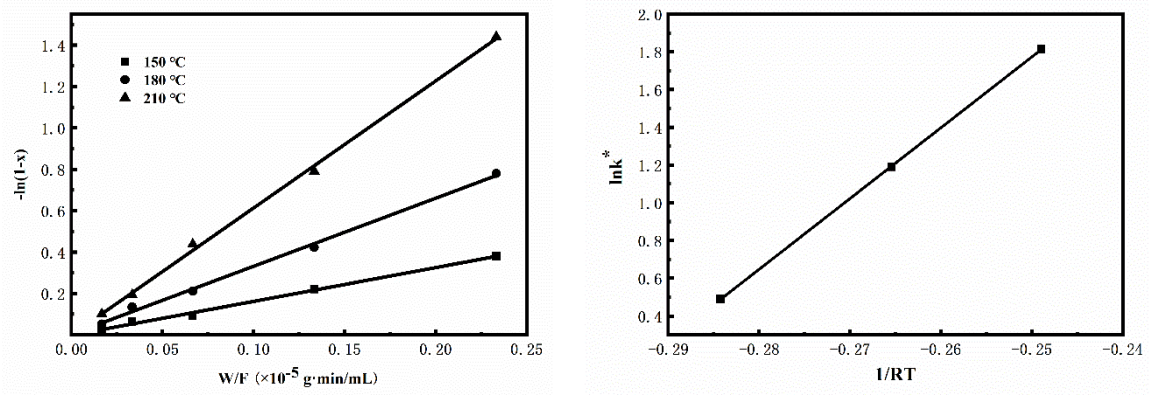

Figure 3. (**a**) First-order reaction of NO result from which to determine the apparent reaction constant, and (**b**) Arrhenius plot from which to determine the apparent activation energy.

The apparent activation energy of Mn10Ce41/NG catalyst in the SCR reaction is determined as 37.6 kJ/mol. This value is much lower than other catalysts such as Fe-ZSM-5 (54 kJ/mol) [31] and Fe-Mo/ZSM-5 (65.16 kJ/mol) [34]. The kinetic analysis demonstrates that the catalytic activity of Mn10Ce41/NG is much higher than of many others.

In addition to kinetic analyses, we have further determined the optimal processing conditions to maximize the de-nitration efficiency on the novel Mn10Ce41/NG catalyst.

The SCR denitrification efficiency of Mn10Ce41/NG catalyst as a function of O_2 concentration were investigated at 150 °C and 180 °C, respectively. As seen in Figure 4, at a low O_2 concentration level, the denitrification efficiency increased rapidly but gradually leveled off with increasing the O_2 concentration. As oxygen concentration is 3% or higher, the denitrification efficiency remains constant. These results are consistent with the kinetic analyses. Oxygen molecules will absorb and dissociate into an O^- activated state on Ce^{3+} sites via charge transfer. The surface activated oxygen species are crucial for promoting the reaction between NO and NH_3. However, there must be a saturation state determined by the area of catalyst surface. More oxygen supply has no benefits for NO conversion, but is a waste of resources.

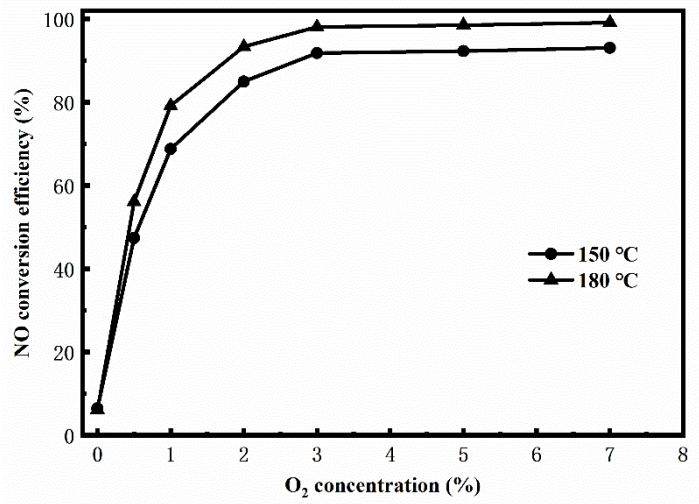

Figure 4. Effect of O_2 concentration on NO conversion of Mn10Ce41/NG catalyst.

Figure 5 shows the NO reduction efficiency as a function of the molar ratio between ammonia and nitrogen ($n_{[NH3]}/n_{[NO]}$). Again, the NO conversion rate increased rapidly with the increase in reductant NH_3 concentration at the low level of $n_{[NH3]}/n_{[NO]}$. As

$n_{[NH3]}/n_{[NO]}$ = 1.0, the NO conversion rate is saturated and does not change with the increase in NH_3 concentration in the reaction gas. The kinetic analysis shows that the rate-determining rate of the NH_3-SCR reaction on Mn10Ce41/NG is the charge transfer of adsorbed NO and O_2 on the catalyst's active sites. Even though the reaction between nitrite-adsorbed NH_4^+ is kinetically faster, NH_3 is desired as the reductant gas for the selective reduction, and the molar ratio between NH_3 and NO determines the steady-state NO conversion result. At the low concentration of NH_3 in the reaction gas, the amount of NH_3 adsorbed onto the catalyst surface is proportional to the amount of NH_3 in the flue gas. The stoichiometry of the NH_3-SCR (see eq 1) demands the value $n_{[NH3]}/n_{[NO]}$ = 1.

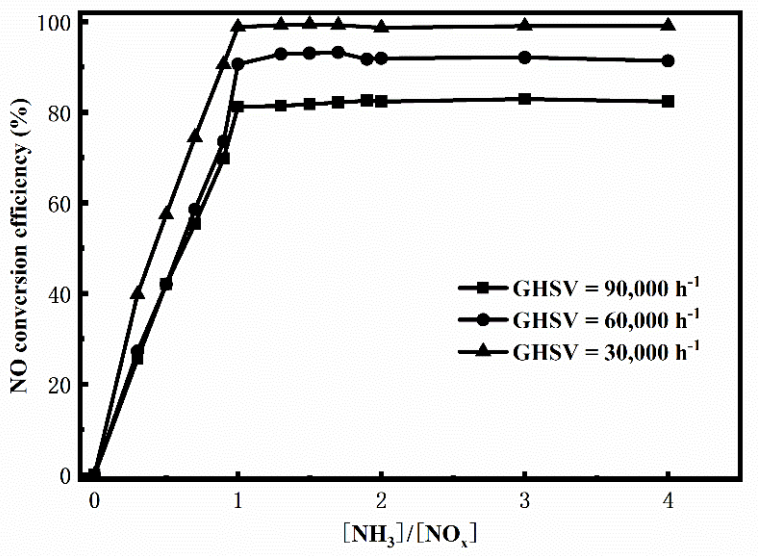

Figure 5. Effects of $n_{[NH3]}/n_{[NO]}$ on NO conversion efficiency of Mn10Ce41/NG catalyst.

With a further increase the concentration of NH_3 in the reaction gas beyond the unity, the excessive NH_3 gas cannot react with NO. The fact that NO's conversion efficiency did not decrease with the increase in $n_{[NH3]}/n_{[NO]}$ indicates no side reaction related to NH_3 or NO occurred at 180 °C. However, if NH_3 is supplied at more than reaction, the excessive NH_3 will be present at the exit gas port. If it was fed to the following dust collector and desulfurization tower, the NH_3 residue will react with SO_2 and H_2O, producing sulfate particulate which will block and corrode the tail gas pipe. Therefore, it is recommended that the value of $n_{[NH3]}/n_{[NO]}$ in SCR on NGMn10Ce41 is set at 1.0.

Figure 6 shows the NO conversion efficiencies of the catalyst Mn10Ce41/NG at various GHSV (15,000–90,000 h^{-1}, corresponding to 500–3000 mL/min of total flow rate) in the temperature range of 150–210 °C. At 150 °C, the denitrification efficiency gradually falls as GHSV increases. As the reaction temperature rises, the impact of GHSV on the catalyst's NO conversion is insignificant. At low reaction temperatures, SCR reaction kinetics on the catalyst surface are relatively slow. Lower GHSV will be beneficial to extend the reaction gas's interaction time with the catalyst. As the temperature is increased, the catalyst's SCR activity increases, and a shorter contact time is sufficient to achieve a higher NO conversion rate. The NO conversion efficiency is less sensitive to the flue gas flow rate within an appropriate range. Although low GHSV will increase the contact time, benefiting denitrification to a certain extent, too low a GHSV will increase resistance to the external diffusion of reaction products and possibly lead to the occurrence of side reactions related to ammonia, hence resulting in a decrease in the denitrification efficiency of the catalyst.

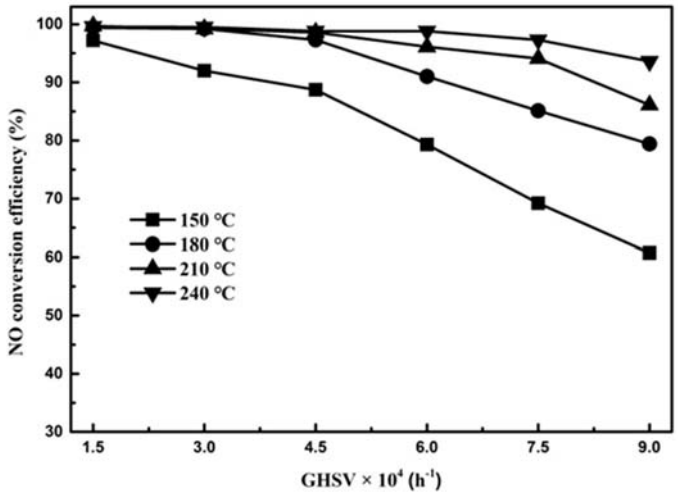

Figure 6. Effect of reaction temperature and GHSV on denitrification efficiency of NG-Mn10Ce41 catalyst.

As seen in Figure 6, on the Mn10Ce41/NG catalyst, the NO convention efficiency is nearly 100% at $n_{[NH3]}/n_{[NO]}$ = 1 with 3–5% O_2 under GHSV of 15,000–30,000 h^{-1} at 180–210 °C. Even at 150 °C, the denitration efficiency can reach 97%. In our previous studies, Mn10Ce41 supported on graphene aerogel shows only 80% NO conversion at 150 °C [yz]. Apparently, when using N-doped graphene as catalyst carrier, the catalytic activities at low temperatures are dramatically improved. The N-doped graphene carrier may provide extra active sites for oxygen absorption, and/or its distinguished electrical properties promote charge transfer among absorbed species and active catalyst nanoparticles.

4. Conclusions

In this study, we have developed a novel MnO_x-CeO_2 nanocomposite on nitrogen-doped graphene nanosheets, i.e., Mn(X)Ce(Y)/NG, among which Mn10Ce41/NG exhibits the best catalytic activity for a low-temperature NH_3-SCR reaction. Kinetic studies have determined that the reaction orders of NO, NH_3 and O_2 are 1, 0 and nearly 1/3~1/2, respectively. This confirms that the L–H mechanism mainly controls the NH_3-SCR on Mn10Ce41/NG, similar to those MnO_x-CeO_2 catalysts on oxide supporters. However, the apparent activation energy in SCR reaction is 37.6 kJ/mol, much lower than the others, which may benefit from the nano-sized active catalyst as well as the N-doped graphene carrier which provides more active sites and charge transfer. To maximize the NO conversion efficiency at low temperatures (150 °C to 210 °C), key processing parameters such as O_2 concentration, NH_3/NO mole ratio, and gas hourly space velocity need to be optimized. Specifically for this studied system, it is determined that the NO convention efficiency is nearly 100% at $n_{[NH3]}/n_{[NO]}$ = 1 with 3–5% O_2 under GHSV of 15,000–30,000 h^{-1} at 180–210 °C. Even at 150 °C, the de-nitration efficiency can reach 97%. The low activation energy and high NO conversion efficiency consistently demonstrate that Mn10Ce41/NG is a promising candidate for low-temperature NH_3-SCR applications. Its stabilities at higher temperatures and in the presence of poisonous gases will be investigated in the near future.

Author Contributions: Formal analysis, S.T.; data curation and writing-original draft, Z.Y.; writing-review & editing, H.H.; conceptualization, F.L.; investigation, Z.L.; resources, X.W. All authors have read and agreed to the published version of the manuscript.

Funding: This work was supported by National Natural Science Foundation of China (62073134).

Data Availability Statement: Data are contained within the article.

Conflicts of Interest: The authors declare no conflict of interest.

References

1. Nova, I.; Lietti, L.; Tronconi, E.; Forzatti, P. Dynamics of SCR reaction over a TiO_2-supported vanadia–tungsta commercial catalyst. *Catal. Today* **2000**, *60*, 73–82. [CrossRef]
2. Casanova, M.; Rocchini, E.; Trovarelli, A.; Schermanz, K.; Begsteiger, I. High-temperature stability of V_2O_5/TiO_2-WO_3-SiO_2 SCR catalysts modified with rare-earths. *J. Alloys Compd.* **2006**, *408*, 1108–1112. [CrossRef]
3. Shang, X.; Hu, G.; He, C.; Zhao, J.; Zhang, F.; Xu, Y.; Zhang, Y.; Li, J.; Chen, J. Regeneration of full-scale commercial honeycomb monolith catalyst (V_2O_5–WO_3/TiO_2) used in coal-fired power plant. *J. Ind. Eng. Chem.* **2012**, *18*, 513–519. [CrossRef]
4. Qi, C.; Bao, W.; Wang, L.; Li, H.; Wu, W. Study of the V_2O_5-WO_3/TiO_2 Catalyst Synthesized from Waste Catalyst on Selective Catalytic Reduction of NOx by NH_3. *Catalysts* **2017**, *7*, 110. [CrossRef]
5. Yu, J.; Guo, F.; Wang, Y.; Zhu, J.; Liu, Y.; Su, F.; Gao, S.; Xu, G. Sulfur poisoning resistant mesoporous Mn-base catalyst for low-temperature SCR of NO with NH_3. *Appl. Catal. B Environ.* **2010**, *95*, 160–168. [CrossRef]
6. Maitarad, P.; Zhang, D.; Gao, R.; Shi, L.; Li, H.; Huang, L.; Rungrotmongkol, T.; Zhang, J. Combination of Experimental and Theoretical Investigations of $MnO_x/Ce_{0.9}Zr_{0.1}O_2$ Nanorods for Selective Catalytic Reduction of NO with Ammonia. *J. Phys. Chem. C* **2013**, *117*, 9999–10006. [CrossRef]
7. Jiang, B.; Liu, Y.; Wu, Z. Low-temperature selective catalytic reduction of NO on MnO_x/TiO_2 prepared by different methods. *J. Hazard. Mater.* **2009**, *162*, 1249–1254. [CrossRef]
8. Xie, J.; Fang, D.; He, F.; Chen, J.; Fu, Z.; Chen, X. Performance and mechanism about MnO_x species included in MnO_x/TiO_2 catalysts for SCR at low temperature. *Catal. Commun.* **2012**, *28*, 77–81. [CrossRef]
9. Niu, Y.; Shang, T.; Hui, S.; Zhang, X.; Lei, Y.; Lv, Y.; Wang, S. Synergistic removal of NO and N_2O in low-temperature SCR process with MnOx/Ti based catalyst doped with Ce and V. *Fuel* **2016**, *185*, 316–322. [CrossRef]
10. Qi, G.; Yang, R.T.; Chang, R. MnO_x-CeO_2 mixed oxides prepared by co-precipitation for selective catalytic reduction of NO with NH_3 at low temperatures. *Appl. Catal. B Environ.* **2004**, *51*, 93–106. [CrossRef]
11. Jin, R.; Liu, Y.; Wu, Z.; Wang, H.; Gu, T. Relationship between SO_2 poisoning effects and reaction temperature for selective catalytic reduction of NO over Mn–Ce/TiO_2 catalyst. *Catal. Today* **2010**, *153*, 84–89. [CrossRef]
12. Qiu, L.; Pang, D.; Zhang, C.; Meng, J.; Zhu, R.; Ouyang, F. In situ IR studies of Co and Ce doped Mn/TiO_2 catalyst for low-temperature selective catalytic reduction of NO with NH_3. *Appl. Surf. Sci.* **2015**, *357*, 189–196. [CrossRef]
13. Wu, Z.; Jin, R.; Liu, Y.; Wang, H. Ceria modified MnO_x/TiO_2 as a superior catalyst for NO reduction with NH_3 at low-temperature. *Catal. Commun.* **2008**, *9*, 2217–2220. [CrossRef]
14. Boningari, T.; Ettireddy, P.R.; Somogyvari, A.; Liu, Y.; Vorontsov, A.; McDonald, C.A.; Smirniotis, P.G. Influence of elevated surface texture hydrated titania on Ce-doped Mn/TiO_2 catalysts for the low-temperature SCR of NO_x under oxygen-rich conditions. *J. Catal.* **2015**, *325*, 145–155. [CrossRef]
15. Cao, F.; Xiang, J.; Su, S.; Wang, P.; Sun, L.; Hu, S.; Lei, S. The activity and characterization of MnO_x–CeO_2–ZrO_2/γ-Al_2O_3 catalysts for low temperature selective catalytic reduction of NO with NH_3. *Chem. Eng. J.* **2014**, *243*, 347–354. [CrossRef]
16. Cao, F.; Xiang, J.; Su, S.; Wang, P.; Hu, S.; Sun, L. Ag modified Mn–Ce/γ-Al_2O_3 catalyst for selective catalytic reduction of NO with NH_3 at low-temperature. *Fuel Process. Technol.* **2015**, *135*, 66–72. [CrossRef]
17. Cao, F.; Su, S.; Xiang, J.; Wang, P.; Hu, S.; Sun, L.; Zhang, A. The activity and mechanism study of Fe–Mn–Ce/γ-Al_2O_3 catalyst for low temperature selective catalytic reduction of NO with NH_3. *Fuel* **2015**, *139*, 232–239. [CrossRef]
18. Luo, J.Z.; Gao, L.Z.; Leung, Y.L.; Au, C.T. The decomposition of NO on CNTs and 1 wt% Rh/CNTs. *Catal. Lett.* **2000**, *66*, 91–97. [CrossRef]
19. Long, R.Q.; Yang, R.T. Carbon Nanotubes as a Superior Sorbent for Nitrogen Oxides. *Ind. Eng. Chem. Res.* **2001**, *40*, 4288–4291. [CrossRef]
20. Su, Y.; Fan, B.; Wang, L.; Liu, Y.; Huang, B.; Fu, M.; Chen, L.; Ye, D. MnO_x supported on carbon nanotubes by different methods for the SCR of NO with NH_3. *Catal. Today* **2013**, *201*, 115–121. [CrossRef]
21. You, X.; Sheng, Z.; Yu, D.; Yang, L.; Xiao, X.; Wang, S. Influence of Mn/Ce ratio on the physicochemical properties and catalytic performance of graphene supported MnO_x-CeO_2 oxides for NH_3-SCR at low temperature. *Appl. Surf. Sci.* **2017**, *423*, 845–854. [CrossRef]
22. Yang, L.; You, X.; Sheng, Z.; Ma, D.; Yu, D.; Xiao, X.; Wang, S.J.N.J.o.C. The promoting effect of noble metal (Rh, Ru, Pt, Pd) doping on the performances of MnO_x–CeO_2/graphene catalysts for the selective catalytic reduction of NO with NH_3 at low temperatures. *New J. Chem.* **2018**, *42*, 11673–11681. [CrossRef]
23. Yao, Z.; Guo, Y.; Yang, Y.; Huang, H.; Qu, D.J. MnO_x-CeO_x nanoparticles supported on graphene aerogel for selective catalytic reduction of nitric oxides. *J. Nanomater.* **2019**, *2019*, 4239764. [CrossRef]
24. Tong, Z.; Lu, X.; Song, C. The CeO_x and MnO_x nanocrystals supported on TiO_2–graphene oxide catalysts and their selective catalytic reduction properties at low temperature. *Crystals* **2017**, *7*, 159. [CrossRef]
25. Zhao, C.; Wu, Y.; Liang, H.; Chen, X.; Tang, J.; Wang, X. N-doped graphene and TiO_2 supported manganese and cerium oxides on low-temperature selective catalytic reduction of NOx with NH3. *J. Adv. Ceram.* **2018**, *7*, 197–206. [CrossRef]
26. Li, X.-F.; Lian, K.-Y.; Liu, L.; Wu, Y.; Qiu, Q.; Jiang, J.; Deng, M.; Luo, Y. Unraveling the formation mechanism of graphitic nitrogen-doping in thermally treated graphene with ammonia. *Sci. Rep.* **2016**, *6*, 23495. [CrossRef] [PubMed]
27. Kim, H.; Lee, K.; Woo, S.I.; Jung, Y. On the mechanism of enhanced oxygen reduction reaction in nitrogen-doped graphene nanoribbons. *Phys. Chem. Chem. Phys.* **2011**, *13*, 17505–17510. [CrossRef] [PubMed]

28. Li, J.; Zhang, Y.; Zhang, X.; Han, J.; Wang, Y.; Gu, L.; Zhang, Z.; Wang, X.; Jian, J.; Xu, P.; et al. Direct transformation from graphitic C3N4 to nitrogen-doped graphene: An efficient metal-free electrocatalyst for oxygen reduction reaction. *ACS Appl. Mater. Interfaces* **2015**, *7*, 19626–19634. [CrossRef] [PubMed]
29. Hummers Jr, W.S.; Offeman, R.E. Preparation of graphitic oxide. *J. Am. Chem. Soc.* **1958**, *80*, 1339. [CrossRef]
30. Cheekati, S.; Xing, Y.; Zhuang, Y.; Huang, H. Graphene platelets and their manganese composites for lithium-ion batteries. *ECS Trans.* **2011**, *33*, 23. [CrossRef]
31. Huang, H.Y.; Long, R.Q.; Yang, R.T. Kinetics of selective catalytic reduction of NO with NH_3 on Fe-ZSM-5 catalyst. *Appl. Catal. A Gen.* **2002**, *235*, 241–251. [CrossRef]
32. Kijlstra, W.S.; Brands, D.S.; Poels, E.K.; Bliek, A. Mechanism of the Selective Catalytic Reduction of NO by NH_3 over MnO_x/Al_2O_3. *J. Catal.* **1997**, *171*, 208–218. [CrossRef]
33. Bosch, H.; Janssen, F.J.; van den Kerkhof, F.M.; Oldenziel, J.; van Ommen, J.G.; Ross, J.R. The activity of supported vanadium oxide catalysts for the selective reduction of NO with ammonia. *Appl. Catal.* **1986**, *25*, 239–248. [CrossRef]
34. Høj, M.; Beier, M.J.; Grunwaldt, J.-D.; Dahl, S. The role of monomeric iron during the selective catalytic reduction of NO_x by NH_3 over Fe-BEA zeolite catalysts. *Appl. Catal. B Environ.* **2009**, *93*, 166–176. [CrossRef]

Disclaimer/Publisher's Note: The statements, opinions and data contained in all publications are solely those of the individual author(s) and contributor(s) and not of MDPI and/or the editor(s). MDPI and/or the editor(s) disclaim responsibility for any injury to people or property resulting from any ideas, methods, instructions or products referred to in the content.